Large-scale shell-model study for excitations across the neutron $N = 82$ shell gap in $^{131-133}$Sb

Han-Kui Wang,[1,*] S. K. Ghorui,[2,3] Kazunari Kaneko,[4] Yang Sun,[2,3,5,6,†] and Z. H. Li[6]

[1]*College of Physics and Telecommunication Engineering, Zhoukou Normal University, Henan 466000, People's Republic of China*
[2]*School of Physics and Astronomy, Shanghai Jiao Tong University, Shanghai 200240, China*
[3]*Collaborative Innovation Center of IFSA, Shanghai Jiao Tong University, Shanghai 200240, China*
[4]*Department of Physics, Kyushu Sangyo University, Fukuoka 813-8503, Japan*
[5]*Institute of Modern Physics, Chinese Academy of Sciences, Lanzhou 730000, China*
[6]*China Institute of Atomic Energy, P.O. Box 275(10), Beijing 102413, China*

(Received 21 July 2017; revised manuscript received 21 October 2017; published 15 November 2017)

The cross-shell excitations in the mass-130 region are determined by the behavior of the single-particle (or single-hole) states around the doubly magic nucleus ^{132}Sn and the size of the energy gaps at $N = 82$ and/or $Z = 50$. The present work reports on the results from large-scale shell-model calculations with the extended paring plus quadrupole-quadrupole force, usually with additions of monopole corrections (the EPQQM model). This paper applies the EPQQM model to the northwestern quadrant of ^{132}Sn. The model space includes the orbits of $(0g_{7/2}, 1d_{5/2}, 1d_{3/2}, 2s_{1/2}, 0h_{11/2})$ for both protons and neutrons, with two additional neutron orbits $(1f_{7/2}, 2p_{3/2})$ above the $N = 82$ shell gap, allowing cross-shell excitations. It is found that the experimentally known low-lying levels for ^{133}Sb, ^{132}Sb, and ^{131}Sb can be well described. The highly excited states above 4.0 MeV are clearly explained as excitations across the neutron $N = 82$ shell gap. The monopole effects in these nuclei are carefully examined. In contrast to the already studied northeastern and southwestern quadrants around ^{132}Sn by the EPQQM model, the description of the current Sb data does not request particular monopole corrections. Experiments to further explore the cross-shell excitations in the Sb isotopes are called for.

DOI: 10.1103/PhysRevC.96.054313

I. INTRODUCTION

The structure of the neutron-rich nuclei in the $A = 130$ mass region is an interesting topic for both nuclear physics and nuclear astrophysics. Recently, there have been a number of experiments performed at the world-reknown facilities. The doubly magic nature of ^{132}Sn has been reconfirmed by studying various physical quantities, such as by measuring a direct Penning trap mass [1], through a direct observation of single-particle states in its neighboring odd-mass isotopes [2,3], and by studying collectivity evolution in the neutron-rich Pd isotopes by measurements of the low-lying excited states [4]. The validity of seniority near ^{132}Sn, a strong signal of shell closure, was found through experimental observation of 8^+ seniority isomeric states in ^{126}Pd, ^{128}Pd, and ^{130}Cd [5,6] and discussed with shell-model calculations [7].

Historically, in the study of the r-process nucleosynthesis, the classical $N = 82$ waiting-point nucleus ^{130}Cd was first identified by Kratz *et al.* in 1986 [8]. It was shown that there is a strong correlation between the $N = 82$ shell closure and the $A \approx 130$ peak of the solar r-process abundance distribution, and therefore, structural information of the nuclei near ^{132}Sn is of crucial importance in understanding the detailed nucleosynthesis steps in the r-process [5].

Near a doubly closed-shell nucleus, the excited spectra are usually recognized as consisting of two types of excitations: excitations of valence single particles and those across the shell gap(s). It is worthwhile to mention that excitations across the neutron $N = 82$ shell gap may be important for understanding the missing β-decay strength when the $N = 82$ waiting-point nuclei are discussed. In a very recent example of β decays in ^{130}Cd [9], the excitation scheme of ^{130}In in the energy intervals 3.5–4.3 and 5.2–5.6 MeV were observed. These states were expected to involve excitations across the neutron $N = 82$ shell gap. These high-energy excited states contain valuable information on the shell evolution. However, owing to their complicated coupling structure of the low-lying single-particle (hole) states with those above the shell gap(s), it has been a great challenge for theoretical descriptions.

On the theory side, there have been successful shell-model calculations for the nuclei near closed shells. These calculations may be divided into two classes, treating, respectively, the above-mentioned two types of excitations. The low-energy states were studied microscopically with the effective interaction derived, for example, from the CD-Bonn NN potential. The interaction has been proven remarkably successful for describing the low-energy states (see, for examples, Refs. [10–12]). On the other hand, the high-energy (and often high-spin) states of cross-shell excitations were simply interpreted with empirical nucleon-nucleon interactions [13–17]. Because of the separated treatment for the two excitation modes, the interplay between the low-lying, coupled single-particle states and highly excited cross-shell states could not be studied as a whole. It is thus much desired to have a unified treatment for the two types of excited states in a tractable shell-model calculation. The main challenge [18] is to find out a suitable effective shell-model interaction that works for the description of both types of excitations simultaneously.

It has been shown that for the neutron-rich nuclei near ^{132}Sn, the extended paring plus quadrupole-quadrupole force with monopole corrections model (EPQQM) [19–22] can be applied to describe both low-lying states and cross-shell

*Corresponding author: whk2007@163.com
†Corresponding author: sunyang@sjtu.edu.cn

excitations in a consistent manner. In recent publications [7,18,23–25], the level spectra of the neutron-rich nuclei, with a few particles and/or a few holes with respect to ^{132}Sn, have been studied by using the EPQQM Hamiltonian. The interplay between the single-particle (single-hole) and cross-shell excited states in these nuclei has been discussed. For example, the validity of the seniority scheme was confirmed through the discussion of the 8^+ seniority isomeric states in ^{126}Pd, ^{128}Pd, and ^{130}Cd, which leads to the conclusion that the shell closure persists at the neutron number $N = 82$ in the neutron-rich region [7]. The evolution of the neutron $N = 82$ shell gap was investigated in calculations along the isotonic chain $N = 82$ with even proton numbers 36–48, allowing excitations across both the $N = 82$ and $Z = 50$ shell gaps [24]. In a recent study, the structures of $A = 129$ hole nuclei below ^{132}Sn, such as ^{129}Sn, ^{129}In, and ^{129}Cd, were discussed with emphasis on the monopole effects and excitations across the neutron $N = 82$ shell gap, and the low-lying levels were predicted in the most exotic nucleus ^{129}Ag [25].

The previous EPQQM studies were concentrated on the northeast [18] and southwest [23] region of ^{132}Sn. On the other hand, there have been accumulated experimental data for the northwestern region, where the nuclei have a few proton particles and a few neutron holes with respect to ^{132}Sn. In nature, the ^{133}Sb, ^{132}Sb, and ^{131}Sb isotopes are synthesized through β decays of the r-process products ^{133}Sn, ^{132}Sn, and ^{131}Sn, respectively. The β-decay Q value, for example, for the ground state of ^{132}Sn is as large as 8 MeV [26]. Thus, in principle, high-energy levels in the daughter ^{132}Sb can be populated, and their structures need to be understood. The advancement in experimental facilities and techniques has allowed one to access these states. As recent examples, by applying the technique of the isochronous mass spectrometry at GSI (Gesellschaft fuer Schwerionenforschung), the core-excited isomer in fully ionized ^{133}Sb has been directly identified by Sun *et al.* [27], which was determined as the $21/2^+$ isomer at 4.56(10) MeV. This opens up a new half-life domain for the storage-ring measurements. Later, by using cold-neutron-induced fission of ^{235}U and ^{241}Pu targets during the EXILL campaign at the ILL (Institut Laue-Langevin) reactor in Grenoble, Bocchi *et al.* further enriched the spectroscopic information by adding a few γ rays on top of the $21/2^+$ isomer in ^{133}Sb [28].

The present article reports the results of large-scale shell-model calculations for three Sb isotopes ^{133,132,131}Sb, with emphasis on the discussion of excitations across the neutron $N = 82$ shell gap. The paper is organized as follows: In Sec. II, we outline the Hamiltonian and shell-model space for the calculations. In Sec. III, the level spectra of ^{133}Sb, ^{132}Sb, and ^{131}Sb are analyzed in detail by the shell-model results. Finally, a summary is made in Sec. IV.

II. THE HAMILTONIAN AND SHELL MODEL SPACES

A. The Hamiltonian

The EPQQM Hamiltonian [19–22] is given in the following proton-neutron (pn) representation [23] as

$$\begin{aligned} H &= H_{\rm sp} + H_{P_0} + H_{P_2} + H_{QQ} + H_{OO} + H_{HH} + H_{\rm mc} \\ &= \sum_{\alpha,i} \varepsilon^i_a c^\dagger_{\alpha,i} c_{\alpha,i} - \frac{1}{2} \sum_{J=0,2} \sum_{ii'} g_{J,ii'} \sum_M P^\dagger_{JM,ii'} P_{JM,ii'} \\ &\quad - \frac{1}{2} \sum_{ii'} \frac{\chi_{2,ii'}}{b^4} \sum_M :Q^\dagger_{2M,ii'} Q_{2M,ii'}: \\ &\quad - \frac{1}{2} \sum_{ii'} \frac{\chi_{3,ii'}}{b^6} \sum_M :O^\dagger_{3M,ii'} O_{3M,ii'}: \\ &\quad - \frac{1}{2} \sum_{ii'} \frac{\chi_{4,ii'}}{b^8} \sum_M :H^\dagger_{4M,ii'} H_{4M,ii'}: \\ &\quad + \sum_{a\leqslant c,ii'} k_{\rm mc}(ia,i'c) \sum_{JM} A^\dagger_{JM}(ia,i'c) A_{JM}(ia,i'c). \quad (1) \end{aligned}$$

Equation (1) consists of the single-particle Hamiltonian ($H_{\rm sp}$), the $J = 0$ and $J = 2$ pairing ($P^\dagger_0 P_0$ and $P^\dagger_2 P_2$), the quadrupole-quadrupole ($Q^\dagger Q$), the octupole-octupole ($O^\dagger O$), the hexadecapole-hexadecapole ($H^\dagger H$) terms, and the monopole corrections ($H_{\rm mc}$). In the pn representation, $P^\dagger_{JM,ii'}$ and $A^\dagger_{JM}(ia,i'c)$ are the pair operators, while $Q^\dagger_{2M,ii'}$, $O^\dagger_{3M,ii'}$, and $H^\dagger_{4M,ii'}$ are the quadrupole, octupole, and hexadecapole operators, respectively, in which i (i') are indices for protons (neutrons). The parameters $g_{J,ii'}$, $\chi_{2,ii'}$, $\chi_{3,ii'}$, $\chi_{4,ii'}$, and $k_{\rm mc}(ia,i'c)$ are the corresponding force strengths, and b is the harmonic-oscillator range parameter. The two-body force strengths that suit the present particle-hole model space are listed in Table I. We note that these force strengths are not exactly the same as those in our previous paper [23] mainly due to different model space for protons. In particular, the $J = 0$ and $J = 2$ pairing force strengths are stronger than those in Ref. [23].

B. The shell-model spaces

The model space employed in the present work includes seven neutron and five proton orbits. The five orbits $(0g_{7/2}, 1d_{5/2}, 1d_{3/2}, 2s_{1/2}, 0h_{11/2})$ lying between the magic numbers 50 and 82 span the model space for proton particles and neutron holes. Two extra neutron orbits above the $N = 82$ shell,$(1f_{7/2}$ and $2p_{3/2})$ are added to allow neutron cross-shell excitations. In order to make the dimension of the configuration space tractable, in the present calculation, only one single neutron is allowed to excite across the $N = 82$ shell gap. Except for the value of the $1/2^+$ level in ^{133}Sb, which is taken following the suggestion in Ref. [29], all the single-

TABLE I. The two-body force strengths (in MeV) used in the present calculation.

ii'	$g_{0,ii'}$	$g_{2,ii'}$	$\chi_{2,ii'}$	$\chi_{3,ii'}$	$\chi_{4,ii'}$
pp	0.136	0.038	0.102	0.032	0.0015
nn	0.117	0.035	0.140	0.004	0.0008
pn	0	0	0.082	0	0.0009

particle (single-hole) states are based on the experimental data of ^{133}Sb (^{131}Sn) for the proton (neutron). The single-particle energies (all in MeV) of the orbits in the 50–82 shell are taken as $\varepsilon^{\nu}_{1d3/2} = -7.342$, $\varepsilon^{\nu}_{0h11/2} = -7.407$, $\varepsilon^{\nu}_{2s1/2} = -7.674$, $\varepsilon^{\nu}_{1d5/2} = -8.996$, and $\varepsilon^{\nu}_{0g7/2} = -9.776$ for neutrons; $\varepsilon^{\pi}_{0g7/2} = -9.668$, $\varepsilon^{\pi}_{1d5/2} = -8.706$, $\varepsilon^{\pi}_{2s1/2} = -7.311$, $\varepsilon^{\pi}_{1d3/2} = -7.228$, and $\varepsilon^{\pi}_{0h11/2} = -6.876$ for protons. For the two extra neutron orbits, which are reserved for neutron excitations across the $N = 82$ shell gap, we take $\varepsilon^{\nu}_{f7/2} = -2.402$ MeV and $\varepsilon^{\nu}_{p3/2} = -1.548$ MeV. The neutron shell gap in ^{132}Sn is thereby calculated to be 4.94 MeV by analyzing the neutron odd-even mass differences. The calculated value is in accordance with the experimental data of 4.9 MeV for neutrons [30].

The shell-model code NUSHELLX@MSU [31] is used for calculations. Before detailed calculations for the ^{133}Sb, ^{132}Sb, and, ^{131}Sb isotopes are performed, the parameters of our shell-model Hamiltonian are tested with the two-neutron hole (^{130}Sn) and two-proton particle (^{134}Te) systems with respect to ^{132}Sn. The known experimental spectra are well reproduced in our shell-model calculations for these two neighboring even-even nuclei ^{134}Te and ^{130}Sn. We found, however, that in order to reproduce precisely the correct ordering and energies for the 6^+, 8^+, and 10^+ states in ^{130}Sn, we need to introduce a modification in the three interaction matrix elements, by the amounts of $\Delta\langle h_{11/2},h_{11/2}|V|h_{11/2},h_{11/2}\rangle^{\nu} = -0.15,-0.15,+0.2$ (MeV) for $J = 6,8,10$, respectively. The effect of the modification will be mentioned later again in the next section.

III. RESULTS AND DISCUSSION

A. ^{133}Sb

^{133}Sb has one proton outside the doubly closed shell in ^{132}Sn. Its low-lying states below 3 MeV are proton single particle in nature. The experimental information on ^{133}Sb was first obtained [32] in 1973 at OSIRIS facility through β decay of ^{133}Sn, and later the low-lying single-proton excitations were identified [33,34]. The core-excited $21/2^+$ isomer in this isotope was first identified using the technique of isochronous mass spectrometry at GSI, Germany [27]. The measured neutral-atom half-life is 17μs, with excitation energy centered at 4.56 MeV with the uncertainty of 100 keV. More recently, using cold-neutron-induced fission of ^{235}U and ^{241}Pu targets at the ILL reactor in Grenoble, France, several γ transitions above the $21/2^+$ isomer in ^{133}Sb have been discovered [28]. These new data, together with the core-excited isomer known before, provide excellent testing examples for our present shell-model calculations.

The calculated energy levels of ^{133}Sb are shown in Fig. 1, which are compared with available experimental data. Except for the calculated level of $3/2^+$ at 2.337 MeV, which is slightly lower than the known experimental one at 2.440 MeV, the single-particle states below 3.0 MeV are reproduced quite well. Just below the $3/2^+$ level, we obtained the first excited $1/2^+$ level at 2.258 MeV, which is mainly due to the input for the neutron $\varepsilon^{\nu}_{2s1/2}$ single-particle energy suggested in Ref. [29]. As shown in Fig. 1, for the high-energy part locating between 4 and 5 MeV, the calculation gives qualitatively

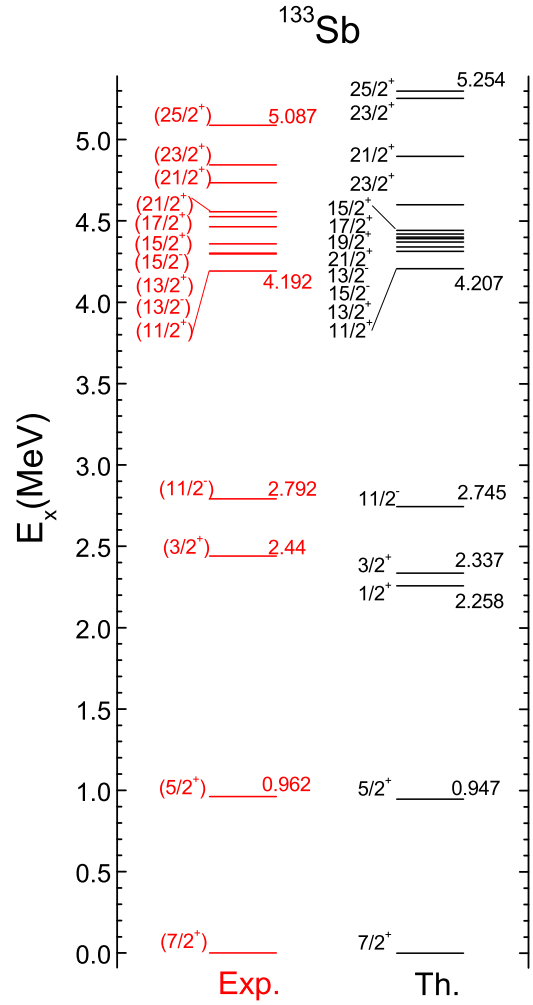

FIG. 1. Comparison of the calculated energy levels with the experimental data for ^{133}Sb. Data are taken from Refs. [15,27,35].

correct results. We now concentrate our discussion on the two lowest configurations for these cross-shell excitations, one with negative parity and another with positive parity.

The levels between 4 and 5 MeV, depicted in Fig. 2, are characterized by the structure of neutron excitations across the $N = 82$ shell gap. In Fig. 2(a), the yrast states belong to the positive-parity configuration $\pi g_{7/2}\nu(h^{-1}_{11/2}f_{7/2})$ are shown, from the lowest possible spin-$11/2^+$ state to the highest $25/2^+$. This configuration describes the states with an excitation of an $h_{11/2}$ neutron below the $N = 82$ shell gap to the $f_{7/2}$ orbit above it. The calculation correctly reproduces the monotonically increasing trend from $11/2^+$ to $15/2^+$ and then suggests a near degeneracy, perhaps a slightly decreasing trend for the $15/2^+$, $17/2^+$, $19/2^+$, and $21/2^+$ states. Experimentally, the highest spin state of this degeneracy group, $21/2^+$, has been identified as a 17-μs isomer [27]. The degeneracy of the $21/2^+$ state with its neighboring lower-spin states explains naturally the formation of the isomerism. We note that our results are of a qualitative difference from the calculation in Ref. [28], which showed essentially an increasing trend for the states from $15/2^+$ to $25/2^+$ of this configuration.

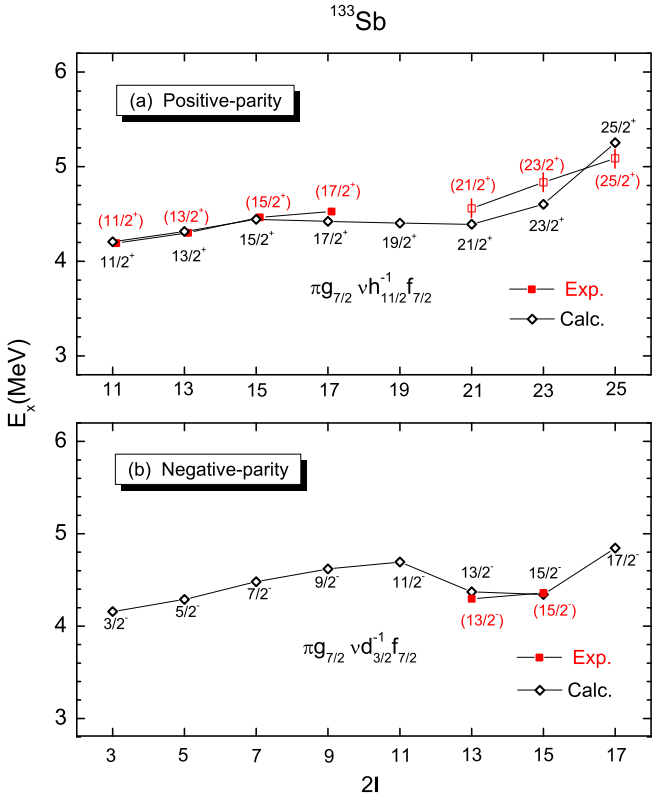

FIG. 2. The calculated levels (opened diamond) of cross-shell excitations in ^{133}Sb, selected from the lowest configuration each for positive parity and negative parity and the lowest energy state for each spin, are compared with available experimental data [35] (filled square). The three experimental levels (opened square) with error bars are taken from Refs. [27,28].

According to our calculation, the states of positive parity shown in Fig. 2(a) all belong to the same configuration of $\pi g_{7/2}\nu(h_{11/2}^{-1}f_{7/2})$. However, different coupling schemes of the angular momenta of the three orbits may yield more than one state for a given total angular momentum, with different energies and wave functions. The coupling of the $h_{11/2}$ neutron hole with the $f_{7/2}$ neutron particle can yield different angular momenta (denoted as νI^{π} hereafter), which further couples with the $\pi g_{7/2}$ proton. For example, the obtained lowest $19/2^+$ level at 4.402 MeV, which is our prediction with no data for comparison, is composed of 22.52% of $[\pi 7/2^+ \bigotimes \nu 6^+]$, 57.54% of $[\pi 7/2^+ \bigotimes \nu 7^+]$, and 19.34% of $[\pi 7/2^+ \bigotimes \nu 8^+]$. There are two $21/2^+$ levels coming out from the calculation. The lower $21/2^+_1$ level calculated at 4.393 MeV, which is close to the experimentally identified 17μs isomer [27], has 31.19% of $[\pi 7/2^+ \bigotimes \nu 7^+]$ and 67.98% of $[\pi 7/2^+ \bigotimes \nu 8^+]$. The second $21/2^+_2$ level, which lies 500 keV above the first one, has mixed configuration of $[\pi 7/2^+ \bigotimes \nu 7^+]$ (68.08%) and $[\pi 7/2^+ \bigotimes \nu 8^+]$ (31.16%). We note that a 208-keV γ ray was recently identified [28], which was suggested to connect the two $21/2^+_1$ levels in ^{133}Sb. There are also two $23/2^+$ levels coming out from the calculation. The lower $23/2^+_1$ level calculated at 4.601 MeV has 87.15% of $[\pi 7/2^+ \bigotimes \nu 8^+]$ and 12.68% of $[\pi 7/2^+ \bigotimes \nu 9^+]$. A 318-keV γ ray was found [28], which was suggested to connect a $23/2^+$ level to the $21/2^+$ isomer. The second $23/2^+_2$ level has 87.32% of $[\pi 7/2^+ \bigotimes \nu 9^+]$ and 12.67% of $[\pi 7/2^+ \bigotimes \nu 8^+]$. The only $25/2^+$ level at 5.254 MeV has pure configuration of $[\pi 7/2^+ \bigotimes \nu 9^+]$, which may be compared with the experimentally identified level with a 561-keV γ ray connecting the $21/2^+$ isomer [28].

The main configuration of the negative-parity states of cross-shell excitations is $\pi g_{7/2}\nu(d_{3/2}^{-1}f_{7/2})$, with more than 82% in purity when seen from the calculation. This configuration corresponds to excitation of an $d_{3/2}$ neutron below the $N = 82$ shell gap to the $f_{7/2}$ orbit above it. In Fig. 2(b), the yrast states belonging to this negative-parity configuration are shown, from the lowest possible spin $3/2^-$ state to the highest $17/2^-$. Experimentally, only two states (with spin parities $13/2^-$ and $15/2^-$) of this configuration are known, for which the calculation shows a remarkable agreement. Interestingly, according to our calculation, these two experimentally identified states locate at the bottom of this yrast sequence, forming an "yrast trap"; see Fig. 2(b). The calculation suggests that the $13/2^-$ level is characterized by substantial mixing of the configurations $[\pi 7/2^+ \bigotimes \nu 3^-]$ (61.25%) and $[\pi 7/2^+ \bigotimes \nu 4^-]$ (21.09%), whereas the $15/2^-$ level has comparably less configuration mixing, 80.6% of $[\pi 7/2^+ \bigotimes \nu 4^-]$ and 7.23% of $[\pi 7/2^+ \bigotimes \nu 5^-]$.

When shell evolution in an exotic mass region is discussed, the influence of the monopole effect on the structure is often an interesting topic. In the previous EPQQM calculations for the nuclei near ^{132}Sn, it has been shown that the monopole correction terms can play significant roles in the determination of the shell structure. The structure of the cross-shell excitation discussed above involves neutron occupations of the $f_{7/2}$ orbit above the $N = 82$ shell gap that are excited from either the $h_{11/2}$ or $d_{3/2}$ orbits below it. Thus it is expected that the monopole correction terms $k_{mc}(\nu h_{11/2}, \nu f_{7/2})$ and $k_{mc}(\nu d_{3/2}, \nu f_{7/2})$ may change the positions of the core-excitation states in a sensitive way.

To illustrate the monopole effect, calculations with inclusion of the monopole correction terms are shown in Fig. 3. It can be seen in Fig. 3(a) that the $k_{mc}(\nu h_{11/2}, \nu f_{7/2})$ term can indeed affect the positive-parity core excited states with the $\pi g_{7/2}\nu(h_{11/2}^{-1}f_{7/2})$ configuration. By varying the strength of $k_{mc}(\nu h_{11/2}, \nu f_{7/2})$ from -0.5 to 0.5 MeV, the energies of all the states belonging to this configuration decrease linearly by about 1 MeV. On the other hand, as expected, the same term does not influence the negative-parity states, which can be clearly seen with the examples for the two states $13/2^-$ and $15/2^-$ in Fig. 3(a). The fact that the calculation with zero monopole correction can already reasonably reproduce the four experimentally confirmed states ($11/2^+$, $13/2^+$, $15/2^+$, and $17/2^+$) leads us to conclude that no monopole correction is necessary as far as the existing data are concerned.

In Fig. 3(b), we show how the other monopole correction term $k_{mc}(\nu d_{3/2}, \nu f_{7/2})$ affects the negative-parity cross-shell configuration of $\pi g_{7/2}\nu(d_{3/2}^{-1}f_{7/2})$. We take the two states with $13/2^-$ and $15/2^-$, for which we have experimental data, as representative examples. The calculation suggests that by varying the strength from -0.5 to 0.5 MeV, the energies of these two nearly degenerate states decrease almost linearly from 4.75 to 3.90 MeV. The calculated line passes through

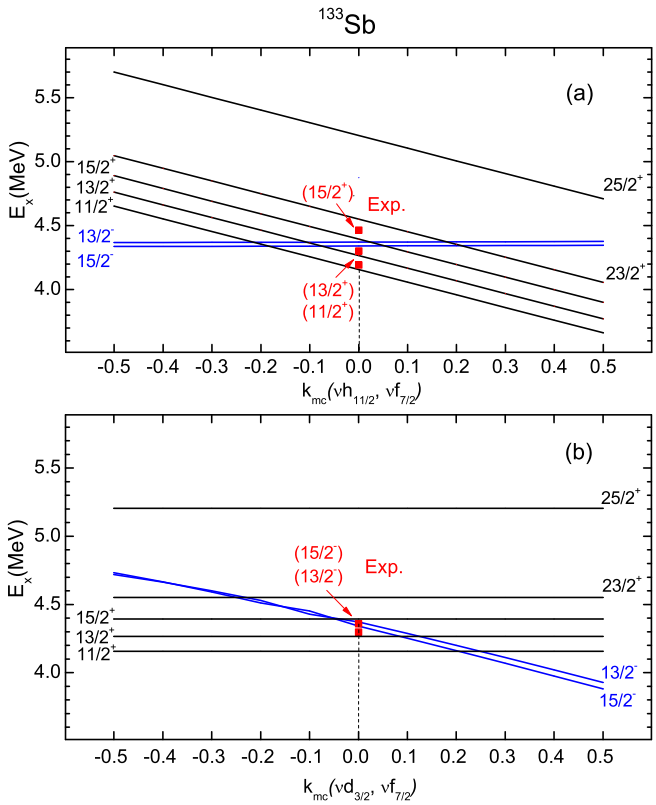

FIG. 3. Illustration of the effects of monopole corrections (a) $k_{mc}(\nu h_{11/2},\nu f_{7/2})$ and (b) $k_{mc}(\nu d_{3/2},\nu f_{7/2})$ on cross-shell excitations in ^{133}Sb. Experimental data points are taken from Ref. [35].

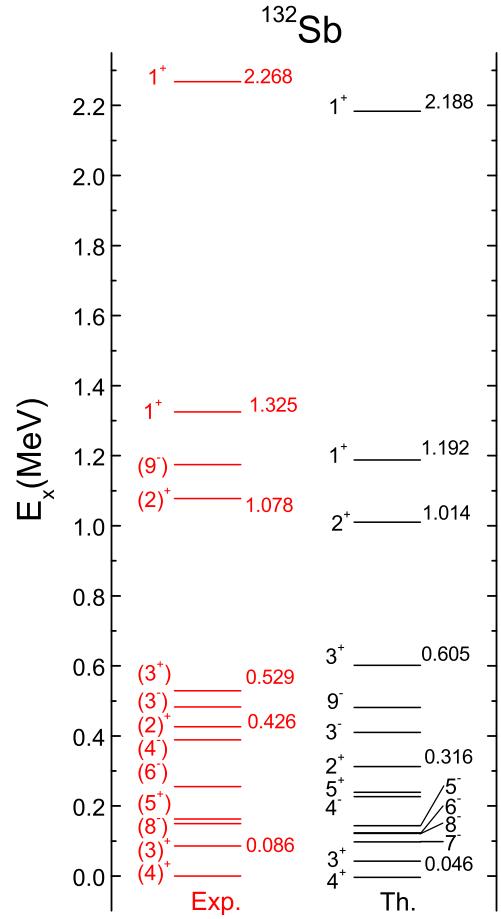

FIG. 4. Comparison of the calculated energy levels with the experimental data in ^{132}Sb. Data are taken from Refs. [35,37,38].

the data points of $13/2^-$ and $15/2^-$ at $k_{mc}(\nu d_{3/2},\nu f_{7/2}) = 0$, suggesting the current experimental information does not suggest necessarily nonzero monopole correction. On the other hand, as expected, the same term does not influence the positive-parity states, which can be clearly seen in Fig. 3(b) with the constant values when the strength parameter varies.

B. ^{132}Sb

The odd-odd isotope ^{132}Sb has its low-lying configurations originating from the coupling of one proton particle in an orbital above the $Z = 50$ shell gap (e.g., $\pi g_{7/2}$) and one neutron hole in an orbital below the $N = 82$ shell gap (e.g., the $\nu h_{11/2}$). Such a coupling scheme makes the spectrum very abundant already at low-lying excitations, and study of them can enhance our understanding about proton-neutron interactions in this mass region. Nearly three decades ago, Stone e*t al.* [36] performed a ^{132}Sn decay measurement and identified much of the low-lying structure of the positive-parity states in ^{132}Sb. It is expected that the lowest configuration for positive-parity states in ^{132}Sb is $\pi g_{7/2}\nu d_{3/2}^{-1}$, whereas for negative-parity states it is $\pi g_{7/2}\nu h_{11/2}^{-1}$. Indeed, our calculation yields the 4^+ ground state of ^{132}Sb with the main configuration of $\pi g_{7/2}\nu d_{3/2}^{-1}$. As illustrated in Fig. 4, the calculated 3^+ level at 0.046 MeV correctly reproduces the experimental 3^+ level at 0.086 MeV, which, along with the 5^+ and 2^+ levels below 0.5 MeV, predominantly has $\pi g_{7/2}\nu d_{3/2}^{-1}$ as the main configuration as of the ground 4^+ state.

The 8^- level is an isomeric state with half-life of $T_{1/2} =$ 4.15 min, which was suggested to be very low in energy, about 0.200 MeV of excitation [39]. This state was estimated in Ref. [36] to be between 0.15 and 0.25 MeV. Our calculation predicts an 8^- level at 0.125 MeV of excitation. This is the lowest negative-parity state in ^{132}Sb with the main configuration of $\pi g_{7/2}\nu h_{11/2}^{-1}$. Our results show that the four levels (with 5^-, 6^-, 7^-, and the above-mentioned 8^- isomer) originating from this configuration are almost degenerate. For the same configuration, there are calculated higher levels including a 4^- level at 0.23 MeV, a 3^- one at 0.414 MeV, and a 2^- one at 0.678 MeV. The problem is the position of the first 9^- level. This is the highest possible spin state of this $\pi g_{7/2}\nu h_{11/2}^{-1}$ configuration, and, within the present model space, this is the only possible 9^- state in the low-energy region. Our calculation shows that the second 9^- level can exist only as a core-excited state at about 3.9 MeV with the configuration of $\pi g_{7/2}\nu(h_{11/2}^{-2} f_{7/2})$. To compare with the only known experimental 9^- level near 1.2 MeV, our calculated 9^- state of the configuration $\pi g_{7/2}\nu h_{11/2}^{-1}$ is too low in energy (see Fig. 4). To resolve this discrepancy, the monopole correction of $k_{mc}(\pi g_{7/2},\nu h_{11/2})$ may pushed up the first 9^- level, but at

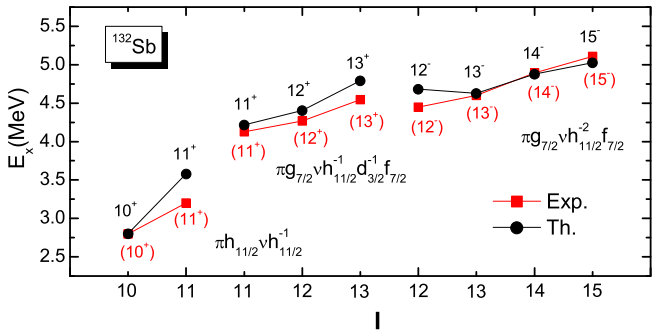

FIG. 5. The experimental high-spin states of ^{132}Sb above 2.5 MeV observed in Ref. [37] and the description of our shell-model calculation with their configurations.

the same time this will also shift other well-described levels 8^-, 6^-,4^-, and 3^- which belong to the same configuration. Another possibility to shift up the 9^- level is to increase aggressively the quadrupole and hexadecapole force between protons and neutrons, but the single-particle states of ^{133}Sb, as well as the low-lying levels of ^{134}Te, would then be poorly described. Thus, theoretical description of the 9^- state in ^{132}Sb remains a puzzle at present. An experimental reinvestigation is much desired.

As for the other low-lying states having a structure from the coupling of one proton particle in an orbit above the $Z = 50$ shell gap and one neutron hole in an orbit below the $N = 82$ shell gap, the calculated 3^+ level at 0.605 MeV with the main configuration of $\pi g_{7/2}\nu s_{1/2}^{-1}$ agrees reasonably with the second experimental 3^+ level at 0.529 MeV. Above 1 MeV of excitation, the experimentally known second 2^+ level at 1.078 MeV and the first 1^+ level at 1.325 MeV correspond well with the calculated 2^+ level at 1.014 MeV and 1^+ level at 1.192 MeV, respectively, both of which are predicted to have the main configuration of $\pi d_{5/2}\nu d_{3/2}^{-1}$. The second experimental 1^+ level at 2.268 MeV may be compared with our calculated 1^+ level at 2.188 MeV, which has the main configuration of $\pi g_{7/2}\nu d_{5/2}^{-1}$. We note that a different configuration (i.e., $\pi d_{5/2}\nu d_{3/2}^{-1}$) was suggested for this state in Ref. [36].

High-energy yrast levels in ^{132}Sb were studied by Bhattacharyya *et al.* in Ref. [37] at Gammasphere using a ^{248}Cm fission source. They were able to identify highly excited states belong to three configurations, $\pi h_{11/2}\nu h_{11/2}^{-1}$, $\pi g_{7/2}\nu(h_{11/2}^{-2}f_{7/2})$, and $\pi g_{7/2}\nu(h_{11/2}^{-1}d_{3/2}^{-1}f_{7/2})$, among which the last two are excited configurations across the $N = 82$ shell. In Fig. 5, some of the calculated yrast levels of these three configurations are depicted and compared with the experimental data reported in Ref. [37]. All the theoretical levels shown here are of more than 90% in purity in the corresponding configurations. For the multiplet of the $\pi h_{11/2}\nu h_{11/2}^{-1}$ configuration, states in the spin range from 0^+ to 11^+ are possible. We note that experimentally, only the two highest spin states (10^+ and 11^+) of this multiplet are identified. Our calculation shows that the lower spin states (not shown in Fig. 5) are either nearly degenerate with the 10^+ one (those with 5^+ to 9^+) or lie higher than this degeneracy group (those with 0^+ to 4^+).

The calculated levels above 4 MeV have a configuration of neutron excitation across the $N = 82$ shell gap. It can be seen from Fig. 5 that the existing experimental data [37] are well reproduced by the shell-model calculations for both positive- and negative-parity levels. The main configuration of the positive-parity levels with spin-parity 11^+ to 13^+ is $\pi g_{7/2}\nu(h_{11/2}^{-1}d_{3/2}^{-1}f_{7/2})$, and the negative-parity levels of 12^- to 15^- have $\pi g_{7/2}\nu(h_{11/2}^{-2}f_{7/2})$ as the dominant configuration. We emphasize that to obtain these results, no monopole correction terms are introduced to Eq. (1). As we have already seen in the previous subsection for ^{133}Sb, the overall satisfactory results for these complicated configurations have been obtained without the need of monopole correction.

C. ^{131}Sb

The structure of low-energy levels in ^{131}Sb is dominated by configurations built by one proton particle and two neutron holes. To compare with ^{133}Sb which has pure proton single-particle levels below 3 MeV, the low-lying spectrum of ^{131}Sb is abundant with many levels due to the addition of two neutron holes. The structure of these states thus becomes complicated. As can be seen in Fig. 6, the experimentally known states below 2.5 MeV are nevertheless reasonably described by the present calculation. The calculation reveals that the ground state $7/2^+$, as well as those positive-parity states lying below 1.5 MeV (including the $3/2^+$, second $5/2_2^+$, $11/2^+$, $9/2^+$, second $7/2_2^+$ states), all have mixed configurations, which are listed in Table II. These levels are mainly made by one $g_{7/2}$ proton coupled with mixture of different neutron-hole pairs. Among them, only the $11/2^+$ level near 1.2 MeV has a relatively pure configuration $\pi g_{7/2}\nu h_{11/2}^{-2}$. The $3/2^+$ level calculated at 1.101 MeV also contains a component from $\pi d_{3/2}\nu h_{11/2}^{-2}$. On the other hand, the first $5/2^+$ level, calculated at 0.906 MeV, has a mixed configuration of one $d_{5/2}$ proton coupled with two different pairs of neutron holes, $\pi d_{5/2}\nu h_{11/2}^{-2}$ and $\pi d_{5/2}\nu d_{3/2}^{-2}$. This calculated level is compared to the experimental $5/2^+$ level at 0.798 MeV. The experimentally known negative-parity levels in ^{131}Sb lie in the excitation from 1.6 to 2.0 MeV, as shown in Fig. 6. The main configuration of these negative-parity levels is found to be $\pi g_{7/2}\nu(h_{11/2}^{-1}d_{3/2}^{-1})$. However, we have to admit that our description can only be qualitatively compared to the data. The calculation fails to obtain the details in the ordering of these negative-parity levels. Recently, the natural parity states for a number of nuclei in this mass region are investigated within the pair-truncated shell-model (PTSM) formalism [41].

There is a known level at 2.392 MeV in experiment with suggested spin parity of $1/2^+$. In our calculation, we found a $1/2^+$ state at 2.366 MeV with a very mixed configuration. The three leading components in the wave function are 40% from $\pi d_{5/2}\nu h_{11/2}^{-2}$, 24% from $\pi s_{1/2}\nu d_{3/2}^{-2}$, and 7% from $\pi s_{1/2}\nu s_{1/2}^{-2}$.

While the low-spin members of the $\pi g_{7/2}\nu h_{11/2}^{-2}$ multiplet were experimentally identified up to the spin $11/2^+$, the higher spin members of this configuration cannot be fed by usual β-decay experiments. In Ref. [40], Genevey *et al.*,

TABLE II. The configuration components (%) in some levels of ^{131}Sb.

Level	E_x (Exp.) (MeV)	E_x (Theo.) (MeV)	$\pi g_{7/2}\nu h_{11/2}^{-2}$	$\pi g_{7/2}\nu d_{3/2}^{-2}$	$\pi g_{7/2}\nu s_{1/2}^{-1}d_{3/2}^{-1}$
$(7/2_1^+)$	0.0	0.0	43.1%	30.3%	
$(3/2^+)$	1.142	1.101	81.1%		
$(5/2_2^+)$	1.203	1.250	80.0%		
$(9/2^+)$	1.229	1.294	29.5%	20.4%	23.0%
$(7/2_2^+)$	1.481	1.487	47.1%	17.8%	15.1%

by using thermal neutron-induced fission of ^{241}Pu, found a high-spin microsecond isomer in ^{131}Sb, a $23/2^+$ isomer at 2.166 MeV. The identification of a 0.096-MeV γ ray led the authors to suggest a $19/2^+$ level at 2.070 MeV. From the analysis of occupation numbers, we obtain that these states have pure configuration of $\pi g_{7/2}\nu h_{11/2}^{-2}$. In Fig. 7(b), we show the members of the $\Delta I = 2$ sequence of this multiplet starting from the ground state $7/2^+$, and compare them with data. Note that there are no experimental data for the $15/2^+$ and $27/2^+$ levels. They are the predictions of our shell-model results.

It is interesting to note that an extra $0g_{7/2}$ proton in ^{131}Sb does not affect much on the smooth behavior in the analogous states in ^{131}Sb when compared with ^{130}Sn. In Fig. 7, we have depicted the analogous states in the $N = 80$ isotones. As one can see, the states in both ^{130}Sn and ^{131}Sb show remarkably similar behaviors. This may suggest a weak coupling scheme of one proton coupled with ^{130}Sn for ^{131}Sb. The exception is the maximally aligned state $27/2^+$ in ^{131}Sb showing a sudden increase in energy, which, however, agrees with the shell-model results using the realistic effective interaction [42,43]. The calculated values of $B(E2)$ are also similar between the states in ^{130}Sn and ^{131}Sb. As we have mentioned earlier, for reproducing the right ordering and energy gap among 6^+, 8^+, and 10^+ levels in ^{130}Sn, we need to modify some of the interaction matrix elements. During our shell-model calculations, we find that the correct ordering and energies of 0^+ to 10^+ levels in ^{130}Sn leads to the corresponding ordering and energies of $7/2^+$ to $27/2^+$ states in ^{131}Sb.

In ^{131}Sb, there have been so far no cross-shell excitations observed experimentally. On the basis of our good description of the high excitations across the neutron $N = 82$ shell gap in ^{133,132}Sb, we predict similar states in ^{131}Sb. As shown in Fig. 8(a), the calculated negative-parity states belonging to the lowest configuration of the cross-shell excitations in ^{131}Sb are shown. This configuration is calculated as $\pi g_{7/2}\nu(h_{11/2}^{-2}d_{3/2}^{-1}f_{7/2})$, which is analogous to the cross-shell negative-parity configuration $\pi g_{7/2}\nu(d_{3/2}^{-1}f_{7/2})$ in ^{133}Sb, as previously discussed in Fig. 2. Same as the coupling scheme of the low-lying states, the structure of this cross-shell configuration in ^{131}Sb is that of ^{133}Sb coupled with an additional neutron-hole pair of $h_{11/2}^{-2}$. We found furthermore that our calculation for ^{131}Sb predicts a local minimum at the spin states of $13/2^-$ and $15/2^-$ [see Fig. 8(a)], which may have a

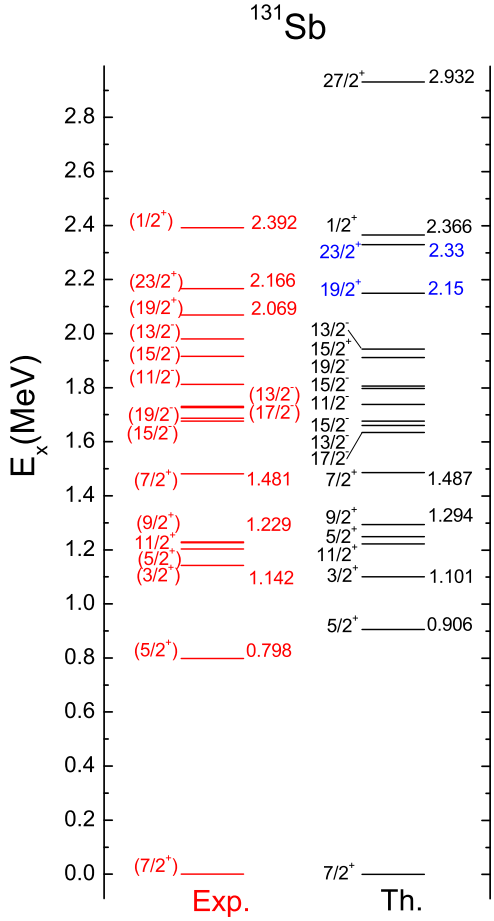

FIG. 6. Comparison of the calculated energy levels with the experimental data in ^{131}Sb. Data are taken from Refs. [35,40].

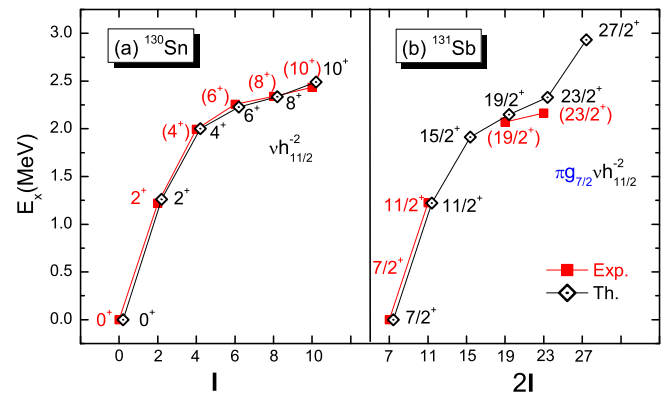

FIG. 7. The levels with $\Delta I = 2$ of (a) the $\nu h_{11/2}^{-2}$ multiplet in ^{130}Sn and (b) the analogous levels of the $\pi g_{7/2}\nu h_{11/2}^{-2}$ multiplet in ^{131}Sb, both of experiment [35,40] and theory.

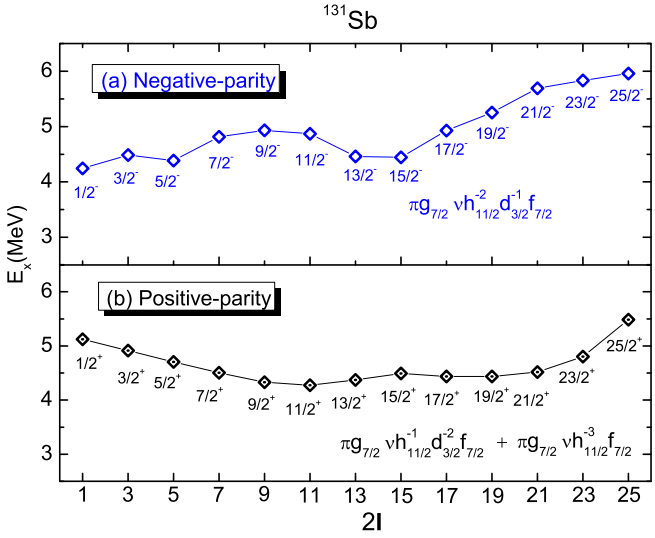

FIG. 8. The calculated levels of cross-shell excitations in ^{131}Sb, selected from the lowest configuration each for positive and negative parity and the lowest energy state for each spin.

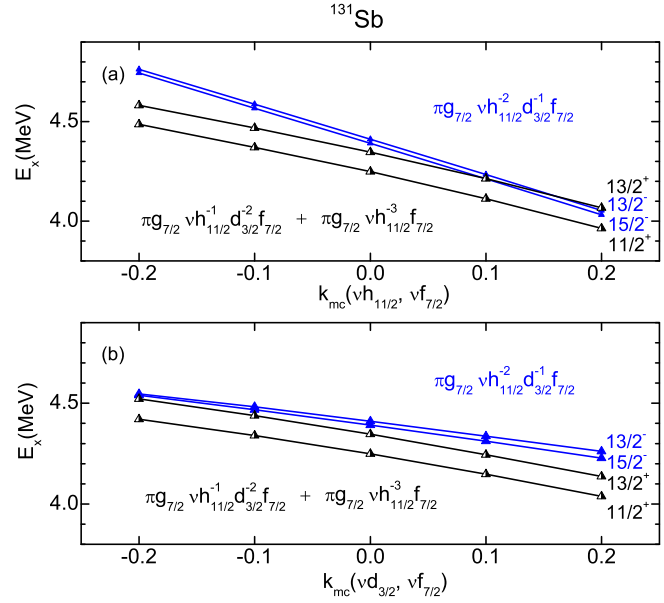

FIG. 9. Illustration of the effects of monopole corrections (a) $k_{mc}(\nu h_{11/2},\nu f_{7/2})$ and (b) $k_{mc}(\nu d_{3/2},\nu f_{7/2})$ on cross-shell excitations in ^{131}Sb.

better possibility to be experimentally observed. As discussed earlier, the corresponding configuration in ^{133}Sb has these two states forming a "yrast trap," which have been the only two states experimentally observed so far for the multiplet.

The lowest positive-parity cross-shell configuration in ^{131}Sb is predicted to have a mixed configurations of $\pi g_{7/2}\nu(h^{-1}_{11/2}d^{-2}_{3/2}f_{7/2})$ and $\pi g_{7/2}\nu(h^{-3}_{11/2}f_{7/2})$. The calculated lowest states of this mixed configuration for each spin are shown in Fig. 8(b). We find that the $11/2^+$ level at 4.273 MeV is the lowest in energy for this configuration. This predicted multiplet may be analogous to the positive-parity cross-shell configuration discussed in Fig. 2(a) for ^{133}Sb.

The structure of the cross-shell excitation discussed in ^{131}Sb involves neutron occupations of the $f_{7/2}$ orbit above the $N = 82$ shell gap that are excited from either the $h_{11/2}$ or $d_{3/2}$ orbits below it. Thus it is again expected that the monopole correction terms $k_{mc}(\nu h_{11/2},\nu f_{7/2})$ and $k_{mc}(\nu d_{3/2},\nu f_{7/2})$ may change the positions of the core-excitation states in a sensitive way. The strengths of the monopole corrections are at present unknown parameters in the shell-model calculation because no such data are available for comparison. Thus it is instructive to perform theoretical calculations to see monopole effects on the cross-shell excitations.

As can be seen in Fig. 9, both of the $k_{mc}(\nu h_{11/2},\nu f_{7/2})$ and $k_{mc}(\nu d_{3/2},\nu f_{7/2})$ terms can indeed affect the core excited states sensitively. Unlike the situation in ^{133}Sb, these two monopole terms give effects on both negative- and positive-parity core excitations. It owes to their more complex configurations, which include all orbitals in these two monopole correction terms. The energies of all these states decrease linearly with the variation of the strength from -0.2 to $+0.2$. Comparing the effects on the states of both parities, the monopole correction $k_{mc}(\nu h_{11/2},\nu f_{7/2})$ [$k_{mc}(\nu d_{3/2},\nu f_{7/2})$] influences the negative-parity states more (less) than the positive-parity states, as shown in Fig. 9.

We finally stress that in the actual calculations for ^{131}Sb shown in Figs. 6, 7(b), and 8, the strength for both monopole corrections, $k_{mc}(\nu h_{11/2},\nu f_{7/2})$ and $k_{mc}(\nu d_{3/2},\nu f_{7/2})$, were set to be zero. This is consistent with the results shown previously for ^{133}Sb and ^{132}Sb, where the calculations without monopole corrections could reproduce the existing data. Any future experimental identification of the cross-shell excited states beyond what have been experimentally known is much desired, as these can suggest how much the monopole corrections are required in this mass region.

D. Electromagnetic transitions

Electromagnetic transitions serve as a strict test for shell-model calculations. For those states having their measured transition rates reported in the literature, we have calculated $E2$ and $M1$ as well as the parity-changing $M2$, $E3$, and $E4$ transition probabilities, which are compared in Table III with available experimental data. The calculations are performed with the standard effective charges of $e_\nu = 0.5e$ for neutrons and $e_\pi = 1.5e$ for protons, and the bare g factors $g_l^\pi = 1$, $g_l^\nu = 0$, $g_s^\pi = 5.586$, and $g_s^\nu = -3.826$, consistent with the early work by our group [18]. It can be seen from Table III that for ^{131}Sb, the theoretical results reproduce the known experimental data well, except for the observed large B ($M4$, $15/2^- \rightarrow 7/2^+$), our calculated value is too small. Also for ^{132}Sb, all the calculated $M1$ and $E2$ for the low-lying, low-spin states are reasonable as compared with the known experimental data. For ^{133}Sb, in addition to the calculation for the two experimentally known parity-changing transition rates, we predict transitions among the states lying below 3 MeV.

In their very recent measurement in ^{133}Sb [28], Bocchi *et al.* reported two $M1$ transition rates among the states of neutron excitations across the $N = 82$ shell gap [see the

TABLE III. Calculated electromagnetic transition probabilities in ^{131,132,133}Sb and compared with the available experimental data [35,40]. Unless a subindex is given, the states mean the lowest one in energy with the same spin and parity.

Transition	τL	Exp. (W.u.)	Th. (W.u.)
^{131}Sb			
$(15/2^-) \to (9/2^+)$	$E3$	0.106 12	0.0139
$(15/2^-) \to (11/2^+)$	$M2$	0.00065 11	0.00023
$(15/2^-) \to (7/2^+)$	$M4$	33 4	0.628
$(19/2^-) \to (15/2^-)$	$E2$	0.99 18	0.913
$(23/2^+) \to (19/2^+)$	$E2$	0.54 11	0.590
^{132}Sb			
$(3)^+ \to (4)^+$	$M1$	0.00112 2	0.0531
$(3)^+ \to (4)^+$	$E2$	0.9 3	2.312
$(2)^+_1 \to (3)^+$	$M1$	0.029 3	0.0322
$(2)^+_1 \to (3)^+$	$E2$	<8.1	0.670
$(2)^+_2 \to (2)^+_1$	$M1$	0.0012 10	0.00004
$(2)^+_2 \to (2)^+_1$	$E2$	0.9 8	0.178
$(2)^+_2 \to (3)^+$	$M1$	0.006 4	0.00037
$(2)^+_2 \to (3)^+$	$E2$	0.9 6	0.220
$1^+ \to (2)^+_2$	$M1$	>0.016	0.485
$1^+ \to (2)^+_2$	$E2$	>0.55	1.717
$1^+ \to (2)^+_1$	$M1$	>0.00034	0.0062
$1^+ \to (2)^+_1$	$E2$	>0.0018	0.0886
^{133}Sb			
$(5/2^+) \to (7/2^+)$	$E2$		0.489
$(3/2^+) \to (5/2^+)$	$M1$		1.631
$(3/2^+) \to (5/2^+)$	$E2$		1.811
$(11/2^+) \to (7/2^+)$	$E2$		0.013
$(11/2^-) \to (5/2^+)$	$E3$	23 12	8.339
$(11/2^-) \to (7/2^+)$	$M2$	0.61 25	7.801

levels in Fig. 2(a)]. These data are valuable because the $M1$ values depend sensitively on the individual orbits, which, in the present case, are below and above the shell gap. Furthermore, the experimental $B(M1)$ values extracted for the $15/2^+ \to 13/2^+$ and $13/2^+ \to 11/2^+$ transitions yield >0.24 W.u. and 0.0042(15) W.u., respectively. As emphasized in Ref. [28], this large difference, of nearly two orders of magnitude, clearly indicates nontrivial changes in structure of the $11/2^+$, $13/2^+$, and $15/2^+$ states. Our calculation suggests that in this energy region with dense levels, two $13/2^+$ and two $15/2^+$ states are involved in the discussion. These four states, together with the $11/2^+$ state below them, all belong to the same configuration of $\pi g_{7/2} \nu(h^{-1}_{11/2} f_{7/2})$. However, as discussed before, the coupling of the $h_{11/2}$ neutron hole with the $f_{7/2}$ neutron particle can yield different angular momenta (denoted as νI^π), which further couple with the $\pi g_{7/2}$ proton. Thus, different coupling schemes of the angular momenta of the three orbits may yield more than one state for a given total angular momentum, with different energies and wave functions. Therefore, the difference in structure among the states with this same configuration is due to different νI^π, resulting from the coupling of one $h_{11/2}$ neutron below and one $f_{7/2}$ neutron above the $N = 82$ gap. We suggest that the

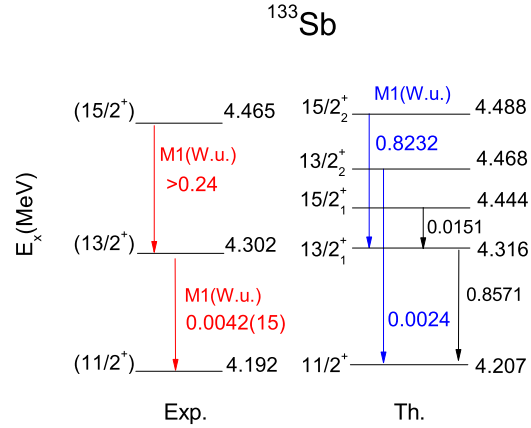

FIG. 10. Schematic illustration of transitions among the three positive-parity states $15/2^+$, $13/2^+$, and $11/2^+$ in ^{133}Sb with the configuration $\pi g_{7/2} \nu(h^{-1}_{11/2} f_{7/2})$. See text for discussion. Experimental data are taken from Ref. [28].

experimentally observed larger $B(M1)$ could correspond to the transition from the calculated second $15/2^+$ to the first $13/2^+$, while the experimentally observed smaller $B(M1)$ could be the one from the second $13/2^+$ to $11/2^+$. Figure 10 illustrates these schematically. Our analysis indicates that in $15/2^+_2$ and $13/2^+_1$, the neutron coupling to $I^\pi = 7^+$ and 8^+ is dominant in both wave functions, and a similar structure is also found in $11/2^+$. In contrast, in $15/2^+_1$ and $13/2^+_2$, the neutron coupling to smaller angular momenta of $I^\pi = 5^+$ and 6^+ are the main components in the wave functions. Thus it is clear that the structures of $15/2^+_2$, $13/2^+_1$, and $11/2^+$ are similar, while those of $15/2^+_1$ and $13/2^+_2$ are similar. Therefore, we obtain a large $B(M1, 15/2^+_2 \to 13/2^+_1) = 0.8232$ for the similar structure in the initial and final states, and a small $B(M1, 13/2^+_2 \to 11/2^+) = 0.0024$ because of the different structure in the initial and final states. These calculated $M1$ values are compared well with the experimental results in Ref. [28]. In addition, a large $B(M1, 13/2^+_1 \to 11/2^+)$ and a small $B(M1, 15/2^+_1 \to 13/2^+_1)$ are predicted; see Fig. 10.

IV. SUMMARY

To summarize, the large-scale shell-model calculations by the EPQQM model, which includes cross-shell excitations, have been performed for some particle-hole nuclei on the northwestern quadrant of ^{132}Sn. The extended paring plus quadrupole-quadrupole force, usually with additions of monopole corrections, has been constructed. The main model space of both protons and neutrons are from the major shell $(0g_{7/2}, 1d_{5/2}, 1d_{3/2}, 2s_{1/2}, 0h_{11/2})$. Furthermore, two additional orbits of $(\nu 1 f_{7/2}, \nu 2 p_{3/2})$ are considered to describe the excitations across the $N = 82$ shell gaps. The neutron shell gap obtained from the neutron odd-even mass differences correctly reproduces the experimental value. Before the application of the model, the Hamiltonian in this model space was tested by comparing it with the experimental low-lying levels of the single-particle nuclei and the two important even-even nuclei of ^{130}Sn and ^{134}Te.

We have shown that the present shell-model results can be successfully applied to describe the level structure of ^{133}Sb, ^{132}Sb, and ^{131}Sb for both low-lying and high-energy states with cross-shell excitation configurations. The main conclusions from the present study are the following.

(1) For all the three Sb isotopes studied here, the level spectrum can be clearly distinguished, with 4 MeV being roughly at the boundary, as of two excitation modes: the low excitations of coupled valence single-particles and high-excitations across the $N = 82$ neutron shell gap. While in ^{133}Sb, levels below 4 MeV are the pure proton single-particle states, those in ^{132,131}Sb in the same excitation region already exhibit complicated structure due to couplings of individual orbits and interactions among them. Of particular interest is those lowest-lying levels which, however, have a structure as a mixture of several configurations. Future measurements of the g factor for this mass region [44,45] may help in providing experimental information on these states.

(2) Highly excited states above 4.0 MeV are explained as excitations across the neutron $N = 82$ shell gap. It has been found that the configurations of the yrast levels of these cross-shell excitations, in all the three isotopes and of both positive and negative parity, involve a $g_{9/2}$ proton coupled with neutron configurations describing an excitation of an $h_{11/2}$ or a $d_{3/2}$ neutron below the $N = 82$ shell gap to the $f_{7/2}$ orbit above it. This simple coupling scheme gives rise to the positive-parity configuration $\pi g_{7/2}\nu(h_{11/2}^{-1} f_{7/2})$ and the negative-parity configuration $\pi g_{7/2}\nu(d_{3/2}^{-1} f_{7/2})$ in ^{133}Sb. The occurrence of an "yrast trap" structure in the yrast sequences may have explained the isomeric characters of the observed states. Similar high-energy excited states in ^{132}Sb can be obtained by adding a neutron $h_{11/2}^{-1}$ hole to those of ^{133}Sb, and high-energy excited states in ^{131}Sb can be obtained by adding a pair of neutron holes of either $h_{11/2}^{-2}$ or $d_{3/2}^{-2}$ to those of ^{133}Sb. We note that experimental measurement of the highly excited states is far from be complete, so a detailed comparison of our calculations with data is impossible at present. Nevertheless, such data are very valuable as they contain information not only to test the shell-model coupling schemes, but also to pin down the size of energy gap(s), which is important for our understanding of the shell evolution in the ^{132}Sn region.

(3) The monopole effects in these nuclei are carefully examined for all the isotopes studied in this paper. In contrast to the already studied examples in the northeastern and southwestern quadrants around ^{132}Sn by the EPQQM model, in which monopole corrections have been found decisive for correct descriptions of certain levels, the current data for these Sb isotopes do not seem to request particular monopole corrections. It should be noted that we have so far only discussed the cross-shell configurations of the yrast sequence for each parities. More experimental data that can further explore the other cross-shell configurations are much desired.

(4) Electromagnetic transition probabilities are calculated for the states with their measured transition rates reported in the literature and are compared in Table III with available experimental data. With the standard effective changes and bare g factors, our calculated $E2$ and $M1$ as well as the parity-changing $M2$, $E3$, and $E4$ transition probabilities compare reasonably well with the known data. We have focused the discussion on the recently observed two $M1$ transitions among the states of neutron excitations across the $N = 82$ shell gap in ^{133}Sb [28]. We have suggested that the remarkably large difference in the two $M1$'s can be explained by the different angular-momentum couplings of the two neutron orbits involved in the cross-shell configuration, one $h_{11/2}$ neutron below and one $f_{7/2}$ neutron above the $N = 82$ shell gap.

ACKNOWLEDGMENTS

Research at Zhoukou Normal University is supported by the National Natural Science Foundation of China (Grant No. 11505302). Research at SJTU is supported by the National Natural Science Foundation of China (Grant No. 11575112), by the National Key Program for S&T Research and Development (Grant No. 2016YFA0400501), and by the 973 Program of China (Grant No. 2013CB834401). Research at China Institute of Atomic Energy is supported by the National Natural Science Foundation of China (Grants No. 11375269 and No. 11490563).

[1] P. Bhattacharyya, P. J. Daly, C. T. Zhang, Z. W. Grabowski, S. K. Saha, R. Broda, B. Fornal, I. Ahmad, D. Seweryniak, I. Wiedenhover *et al.*, Phys. Rev. Lett. **87**, 062502 (2001).

[2] K. L. Jones, A. S. Adekola, D. W. Bardayan, J. C. Blackmon, K. Y. Chae, K. A. Chipps, J. A. Cizewski, L. Erikson, C. Harlin, R. Hatarik *et al.*, Nature (London) **465**, 454 (2010).

[3] K. L. Jones, F. M. Nunes, A. S. Adekola, D. W. Bardayan, J. C. Blackmon, K. Y. Chae, K. A. Chipps, J. A. Cizewski, L. Erikson, C. Harlin *et al.*, Phys. Rev. C **84**, 034601 (2011).

[4] H. Wang, N. Aoi, S. Takeuchi, M. Matsushita, P. Doornenbal, T. Motobayashi, D. Steppenbeck, K. Yoneda, H. Baba, L. Caceres *et al.*, Phys. Rev. C **88**, 054318 (2013).

[5] A. Jungclaus, L. Caceres, M. Gorska, M. Pfutzner, S. Pietri, E. Werner-Malento, H. Grawe, K. Langanke, G. Martinez-Pinedo, F. Nowacki *et al.*, Phys. Rev. Lett. **99**, 132501 (2007).

[6] H. Watanabe, G. Lorusso, S. Nishimura, Z. Y. Xu, T. Sumikama, P.-A. Soderstrom, P. Doornenbal, F. Browne, G. Gey, H. S. Jung *et al.*, Phys. Rev. Lett. **111**, 152501 (2013).

[7] H.-K. Wang, K. Kaneko, and Y. Sun, Phys. Rev. C **89**, 064311 (2014).

[8] K. L. Kratz, H. Gabelmann, W. Hillebrandt, B. Pfeiffer, K. Schlösser, and F.-K. Thielemann, Z. Phys. A **325**, 489 (1986).

[9] A. Jungclaus, H. Grawe, S. Nishimura, P. Doornenbal, G. Lorusso, G. S. Simpson, P.-A. Soderstrom, T. Sumikama, J. Taprogge, Z. Y. Xu *et al.*, Phys. Rev. C **94**, 024303 (2016).
[10] F. Andreozzi, L. Coraggio, A. Covello, A. Gargano, T. T. S. Kuo, and A. Porrino, Phys. Rev. C **56**, R16 (1997).
[11] B. A. Brown, N. J. Stone, J. R. Stone, I. S. Towner, and M. Hjorth-Jensen, Phys. Rev. C **71**, 044317 (2005).
[12] M. P. Kartamyshev, T. Engeland, M. Hjorth-Jensen, and E. Osnes, Phys. Rev. C **76**, 024313 (2007).
[13] B. Fornal, R. Broda, P. J. Daly, P. Bhattacharyya, C. T. Zhang, Z. W. Grabowski, I. Ahmad, D. Seweryniak, I. Wiedenhover, M. P. Carpenter *et al.*, Phys. Rev. C **63**, 024322 (2001).
[14] W. Urban, W. Kurcewicz, A. Korgul, P. J. Daly, P. Bhattacharyya, C. T. Zhang, J. L. Durell, M. J. Leddy, M. A. Jones, W. R. Phillips *et al.*, Phys. Rev. C **62**, 027301 (2000).
[15] W. Urban, A. Zlomaniec, G. S. Simpson, H. Faust, T. Rzaca-Urban, and M. Jentschel, Phys. Rev. C **79**, 037304 (2009).
[16] J. Genevey, J. A. Pinston, H. Faust, C. Foin, S. Oberstedt, and B. Weiss, Eur. Phys. J. A **7**, 463 (2000).
[17] C. T. Zhang, P. Bhattacharyya, P. J. Daly, R. Broda, Z. W. Grabowski, D. Nisius, I. Ahmad, T. Ishii, M. P. Carpenter, L. R. Morss *et al.*, Phys. Rev. Lett. **77**, 3743 (1996).
[18] H. Jin, M. Hasegawa, S. Tazaki, K. Kaneko, and Y. Sun, Phys. Rev. C **84**, 044324 (2011).
[19] M. Hasegawa, K. Kaneko, and S. Tazaki, Nucl. Phys. A **688**, 765 (2001).
[20] K. Kaneko, M. Hasegawa, and T. Mizusaki, Phys. Rev. C **66**, 051306(R) (2002).
[21] K. Kaneko, Y. Sun, M. Hasegawa, and T. Mizusaki, Phys. Rev. C **78**, 064312 (2008).
[22] K. Kaneko, Y. Sun, T. Mizusaki, and M. Hasegawa, Phys. Rev. C **83**, 014320 (2011).
[23] H.-K. Wang, Y. Sun, H. Jin, K. Kaneko, and S. Tazaki, Phys. Rev. C **88**, 054310 (2013).
[24] H.-K. Wang, K. Kaneko, and Y. Sun, Phys. Rev. C **91**, 021303(R) (2015).
[25] H.-K. Wang, K. Kaneko, Y. Sun, Y.-Q. He, S.-F. Li, and J. Li, Phys. Rev. C **95**, 011304(R) (2017).
[26] Yu. Khazov, A. Rodionov, and F. G. Kondev, Nucl. Data Sheets **112**, 855 (2011).
[27] B. Sun, R. Knobelc, H. Geisselac, Yu. A. Litvinov, P. M. Walker, K. Blaum, F. Bosch, D. Boutin, C. Brandau, L. Chen *et al.*, Phys. Lett. B **688**, 294 (2010).
[28] G. Bocchi, S. Leoni, B. Fornal, G. Colo, P. F. Bortignon, S. Bottoni, A. Bracco, C. Michelagnoli, D. Bazzacco, A. Blanc *et al.*, Phys. Lett. B **760**, 273 (2016).
[29] J. Shergur, A. Wohr, W. B. Walters, K.-L. Kratz, O. Arndt, B. A. Brown, J. Cederkall, I. Dillmann, L. M. Fraile, P. Hoff *et al.*, Phys. Rev. C **72**, 024305 (2005).
[30] G. Audi, M. Wang, A. H. Wapstra, F. G. Kondev, M. MacCormick, X. Xu, B. Pfeiffer *et al.*, Chin. Phys. C **36**, 1287 (2012).
[31] B. A. Brown, W. D. M. Rae, E. McDonald, and M. Horoi, Nuclear structure resources (NuShellX@MSU) [http://www.nscl.msu.edu/].
[32] S. Borg, G. B. Holm, and B. Rydberg, Nucl. Phys. A **212**, 197 (1973).
[33] J. Blomqvist, A. Kerek, and B. Fogelberg, Z. Phys. A **314**, 199 (1983).
[34] M. Sanchez-Vega, B. Fogelberg, H. Mach, R. B. E. Taylor, A. Lindroth, and J. Blomqvist, Phys. Rev. Lett. **80**, 5504 (1998).
[35] Data extracted using the NNDC On-line Data Service from the ENSDF database, with cutoff dates of October 31, 2010; February 10, 2005; and July 17, 2006 for ^{133}Sb, ^{132}Sb, and ^{131}Sb, respectively.
[36] C. A. Stone, S. H. Faller, and W. B. Walters, Phys. Rev. C **39**, 1963 (1989).
[37] P. Bhattacharyya, P. J. Daly, C. T. Zhang, Z. W. Grabowski, S. K. Saha, B. Fornal, R. Broda, W. Urban, I. Ahmad, D. Seweryniak *et al.*, Phys. Rev. C **64**, 054312 (2001).
[38] J. K. Hwang, A. V. Ramayya, J. H. Hamilton, C. J. Beyer, J. O. Rasmussen, Y. X. Luo, S. C. Wu, T. N. Ginter, C. M. Folden, III, P. Fallon *et al.*, Phys. Rev. C **65**, 034319 (2002).
[39] A. Kankainen, J. Hakala, T. Eronen, D. Gorelov, A. Jokinen, V. S. Kolhinen, I. D. Moore, H. Penttila, S. Rinta-Antila, J. Rissanen *et al.*, Phys. Rev. C **87**, 024307 (2013).
[40] J. Genevey, J. A. Pinston, H. Faust, C. Foin, S. Oberstedt, and M. Rejmund, Eur. Phys. J. A **9**, 191 (2000).
[41] E. Teruya, N. Yoshinaga, K. Higashiyama, and A. Odahara, Phys. Rev. C **92**, 034320 (2015).
[42] L. Coraggio, A. Covello, A. Gargano, N. Itaco, and T. T. S. Kuo, Phys. Rev. C **66**, 064311 (2002).
[43] L. Coraggio, A. Covello, A. Gargano, N. Itaco, and T. T. S. Kuo, Prog. Part. Nucl. Phys. **62**, 135 (2009).
[44] A. E. Stuchbery, J. M. Allmond, A. Galindo-Uribarri, E. Padilla-Rodal, D. C. Radford, N. J. Stone, J. C. Batchelder, J. R. Beene, N. Benczer-Koller, C. R. Bingham *et al.*, Phys. Rev. C **88**, 051304 (2013).
[45] J. M. Allmond, A. E. Stuchbery, C. Baktash, A. Gargano, A. Galindo-Uribarri, D. C. Radford, C. R. Bingham, B. A. Brown, L. Coraggio, A. Covello *et al.*, Phys. Rev. Lett. **118**, 092503 (2017).